The American Journal of Pathology, Vol. 181, No. 10, October 2012

http://dx.doi.org/10.1016/j.ajpath.2012.06.015

Cardiovascular, Pulmonary, and Renal Pathology

Pressure Overload Induces Early Morphological Changes in the Heart

Colby A. Souders,* Thomas K. Borg,† Indroneal Banerjee,‡ and Troy A. Baudino*§

From the Department of Medicine, Cardiovascular Research Institute, Texas A&M Health Science Center, Temple, Texas; the Department of Regenerative Medicine and Cell Biology,† Medical University of South Carolina, Charleston, South Carolina; the Department of Medicine,‡ University of California-San Diego, San Diego, California; and the Central Texas Veterans Health Care System,§ Temple, Texas*

Cardiac hypertrophy, whether pathological or physiological, induces a variety of additional morphological and physiological changes in the heart, including altered contractility and hemodynamics. Events exacerbating these changes are documented during later stages of hypertrophy (usually termed pathological hypertrophy). Few studies document the morphological and physiological changes during early physiological hypertrophy. We define acute cardiac remodeling events in response to transverse aortic constriction (TAC), including temporal changes in hypertrophy, collagen deposition, capillary density, and the cell populations responsible for these changes. Cardiac hypertrophy induced by TAC in mice was detected 2 days after surgery (as measured by heart weight, myocyte width, and wall thickness) and peaked by day 7. Picrosirius staining revealed increased collagen deposition 7 days after TAC; immunostaining and flow cytometry indicated a concurrent increase in fibroblasts. The findings correlated with angiogenesis in TAC hearts; a decrease in capillary density was observed at day 2, with recovery to sham-surgery levels by day 7. Increased pericyte levels, which were observed 2 days after TAC, may mediate this angiogenic transition. Gene expression suggests a coordinated response in growth, extracellular matrix, and angiogenic factors to mediate the observed morphological changes. Our data demonstrate that morphological changes in response to cardiovascular injury occur rapidly, and the present findings allow correlation of specific events that facilitate these changes. ***(Am J Pathol 2012, 181:1226–1235; http://dx.doi.org/10.1016/j.ajpath.2012.06.015)***

The process of cardiac remodeling is responsible for changes in cardiac morphology and function. Left ventricular hypertrophy, which is observed in response to a variety of pathophysiological signals, is a typical response to pressure overload or any disease state that increases cardiac wall stress and marks an adaptive response to compensate to the unfavorable conditions. Both mechanical and chemical stressors induce cardiac remodeling, and over time the adaptive response concedes to cardiac dilatation and the ensuing remodeling process becomes maladaptive, leading to dysfunction,[1] possibly as a result of enhanced catecholamine chemical signaling by monoamine oxidases.[2] Factors associated with cardiac remodeling include myocyte hypertrophy, increased extracellular matrix (ECM) deposition, and abnormalities of the coronary vasculature.[3,4] The latter two conditions often combine to create perivascular fibrosis, and previous studies have demonstrated that reducing myocardial fibrosis improves coronary hemodynamics.[5] In addition, proliferation of nonmyocyte constituents (ie, fibroblasts, endothelial cells, immune cells, and smooth muscle cells) encourages disorganized tissue heterogeneity,[4] which is initially adaptive but subsequent overcompensation induces pathological cardiac remodeling.[6]

Two principal elements of pathological hypertrophic remodeling that lead to malfunction are accumulation of collagen and vascular remodeling.[7] An increase in collagen deposition stiffens the heart, resulting in systolic and diastolic dysfunction,[8] whereas insufficient angiogenesis deprives the hypertrophic myocardium of oxygenation because of low capillary density.[9–11] Numerous studies have attempted to alter these remodeling processes, with varying success. Some authors have identified a relationship between the degree of hypertrophy and prognosis: higher survival rates were observed in patients treated before left ventricular end systolic diameter reaches 40

Supported in part by NIH grant HL-085847 (T.K.B.) and the American Heart Association (SDG-0830268N to T.A.B. and PRE-3280025 to C.A.S.), with resources and the use of facilities at the Central Texas Veterans Health Care System, Temple, Texas.

Accepted for publication June 20, 2012.

Address reprint requests to Troy A. Baudino, Ph.D., Texas A&M Health Science Center, Cardiovascular Research Institute, 1901 S. 1st St., Bldg. 205, Temple, TX 76504. E-mail: tbaudino@medicine.tamhsc.edu.

mm,[12] thus illustrating the importance of early intervention. Others have succeeded in correlating markers of fibrosis with left ventricular hypertrophy and clinical heart failure,[13,14] indicating that the combination of hypertrophy and fibrosis results in cardiac dysfunction. In addition, it has been shown that treatment to increase capillary density after a pathological insult is accompanied by improved cardiac function, even if delayed treatment is unable to decrease myocardial infarct size,[15] suggesting that capillary density may be more of a determining factor than is tissue remodeling.

One overlooked aspect is the time course within which these changes take place after pathological insult and their progression in relation to each other. Mainly, studies have investigated only later time points (day 7 and later), when advanced stages of remodeling, adaption, and pathology have already manifested in the heart.[16] Limited studies examining early responses to pathology have uncovered important, cell-specific acute responses,[17] but additional research is needed for a better understanding of the immediate response by the heart to injury. In the present study, we analyzed the acute morphological response within the first week after pathological cardiac insult, to determine the early progression of cardiac remodeling and correlate these remodeling events to better understand the complex coordination and how it relates to cardiac function. Here, we illustrate immediate changes in cardiac hypertrophy, angiogenesis, fibrosis, and alterations in the cell populations contributing to these events. We also propose possible gene-specific changes that may guide these morphological changes.

Materials and Methods

Animal Model of Pressure Overload Hypertrophy

Transverse aortic constriction (TAC) was performed in 12-week-old male C57/BL6 mice, as described previously.[18] Mice were anesthetized under 3% isoflurane via intubation, the chest was opened, the aortic arch was visualized, and 6–0 silk suture was passed under the arch between the innominate and left common carotid arteries. The suture was secured around both the aorta and a 28-gauge needle, the needle was removed, the chest was closed, and the mouse was extubated. Sham-surgery mice underwent an identical procedure except for the aortic ligation. Mice were provided buprenorphine via intraperitoneal injection before recovery. Echocardiographic analysis using a Vevo2100 digital imaging system (VisualSonics, Toronto, ON, Canada) was performed under 1% isoflurane at indicated time points (0, 2, 7, 14, and 28 days), with mid ventricle M and B mode measurements acquired in the parasternal short-axis view at the level of the papillary muscles. In addition, echocardiographic analysis and blood pressure measurements were taken before surgery in all animals, to ensure an identical baseline. Adequate levels of anesthesia were monitored by toe pinch, and euthanasia was administered via cervical dislocation under 5% isoflurane. Experiments were approved by the Institutional Animal Care and Use Committee (Scott & White Hospital and Texas A&M Health Science Center) and conform to the Guide for the Care and Use of Laboratory Animals (2011, 8th edition).

Transmission Electron Microscopy

Hearts ($n = 4$) were removed at indicated time points (2, 7, and 28 days) and were flushed in ice-cold PBS. The mid left ventricular free wall and septum were isolated in 4% buffered glutaraldehyde and sectioned into 1-mm blocks. After the initial fixation, samples were postfixed in OsO_4 with 2% tannic acid and then were dehydrated, embedded, and sectioned as described previously.[19] Samples were stained with uranyl acetate and lead hydroxide, and at least four separate grids were imaged for each block with a JEOL 200CX transmission electron microscope at 180 kV (JEOL, Tokyo, Japan). Low-magnification imaging was followed by high-magnification imaging, and representative images were acquired.

Collagen Analysis

Picrosirius-Fast Green staining was modified from a previous protocol.[20] Briefly, heart sections (10 μm) were fixed in 4% paraformaldehyde, stained in a solution of 0.1% Fast Green (Acros; Thermo Fisher Scientific, Pittsburgh, PA) and Sirius Red 0.1% in saturated picric acid (Electron Microscopy Sciences, Hatfield, PA) and imaged at $\times$20 magnification using a Nikon Eclipse TS100 inverted microscope with a Digital Sight DS-2Mv camera and NIS-Elements software version 3.20. Images ($\geq$6 per animal) of mid left ventricle and septum were analyzed using ImageJ software version 1.46 (NIH, Bethesda, MD). The ratio of collagen to total tissue area was calculated.

Immunofluorescent Imaging

Frozen heart sections (10 μm thick) were fixed and immunostained with rat anti-CD31 antibody (BD Pharmingen, San Diego, CA), anti-3G5 antibody isolated from a mouse B-lymphocyte hybridoma cell line (CRL-1814; ATCC, Manassas, VA), and a fibroblast-specific rabbit polyclonal antibody (1611) that was described in a previous report from our laboratory.[21,22] Sections ($\geq$6 per animal) from the mid left ventricle and septum were counterstained with DAPI and phalloidin and then were sequentially imaged under a TCS SP5 white light laser confocal microscope (Leica Microsystems, Wetzlar, Germany) at $\times$40 and $\times$20 magnification. ImageJ software was used for quantitative analysis, and total antibody staining was normalized to DAPI or phalloidin.

Flow Cytometry

Whole hearts from TAC and sham surgery ($n = 4$ each) were prepared at indicated time points (0, 3, 7, and 14 days), as described previously.[23] Briefly, hearts were digested to single-cell suspensions with collagenase and then were labeled with the following antibodies conju-

gated to Qdot nanocrystals (Life Technologies-Invitrogen, Carlsbad, CA), according to the manufacturer's protocol: DDR2 (Santa Cruz Biotechnology, Santa Cruz, CA) for fibroblasts, α-myosin heavy chain (Abcam, Cambridge, MA) for myocytes, CD31 (Zymed Laboratories, South San Francisco, CA) for endothelial cells, and α-smooth muscle actin (R&D Systems, Minneapolis, MN) for vascular smooth muscle cells. An equal number of cells (20,000 events) for each sample were processed using an Epics XL fluorescence-activated cell sorting system (Beckman Coulter, Brea, CA) and were analyzed using the associated Expo 32 software.

Real-Time PCR

Total RNA was extracted at indicated time points (0, 2, and 7 days) from septa and left mid-ventricular regions of TAC and sham-surgery hearts ($n = 4$ each) using an RNeasy Plus mini kit (Qiagen, Valencia, CA) according to the manufacturer's protocol. Isolated RNA was quantified and converted to cDNA with an SABiosciences RT^2 first-strand kit (Qiagen), which was then quantified via quantitative real-time PCR using a StepOnePlus thermocycler (Life Technologies-Applied Biosystems, Foster City, CA). Primer sequences are available upon request.

Statistical Analysis

Echocardiographic, physiological, and immunofluorescent data were analyzed for significance using Student's *t*-test or an analysis of variance test with a Mann-Whitney test. All analyses were performed using Microsoft Excel version 12.3.3 and GraphPad Prism software version 4 (GraphPad Software, La Jolla, CA). Significance was set at $P < 0.05$.

Results

Early Cardiac Growth in TAC Mice

Hearts were examined for gross morphological changes at early (day 2) and late time points (days 7, 14, and 28) after induction of pressure overload by TAC surgery. All animals had similar baseline measurements of cardiac function and blood pressure. Survival rates after TAC were approximately 70% at 28 days after surgery, in accord with findings of similar studies from our laboratory and from others.[18] Echocardiographic analysis revealed a significant increase in relative wall thickness just 48 hours after TAC surgery, which persisted through day 28 (Figure 1A). The ratio of heart weight to body weight also revealed significant cardiac growth in TAC hearts by day 2, and this increased further until by day 7 growth peaked and was maintained through day 28 (Figure 1B). To determine the extent of myocyte hypertrophy during this early growth period, myocyte width was measured in F-actin-stained cross-sections (Figure 1C). Cardiac growth 2 days after TAC cannot be attributed to myocyte growth, because no significant change in myocyte width was measured; however, a significant increase was observed at 7 days after TAC, indicating that myocyte hypertrophy is a contributing factor to the increase in heart weight and wall thickness observed by day 7. Taken together, these data indicate that cardiac growth in response to acute pressure overload is fully realized by day 7 after surgery.

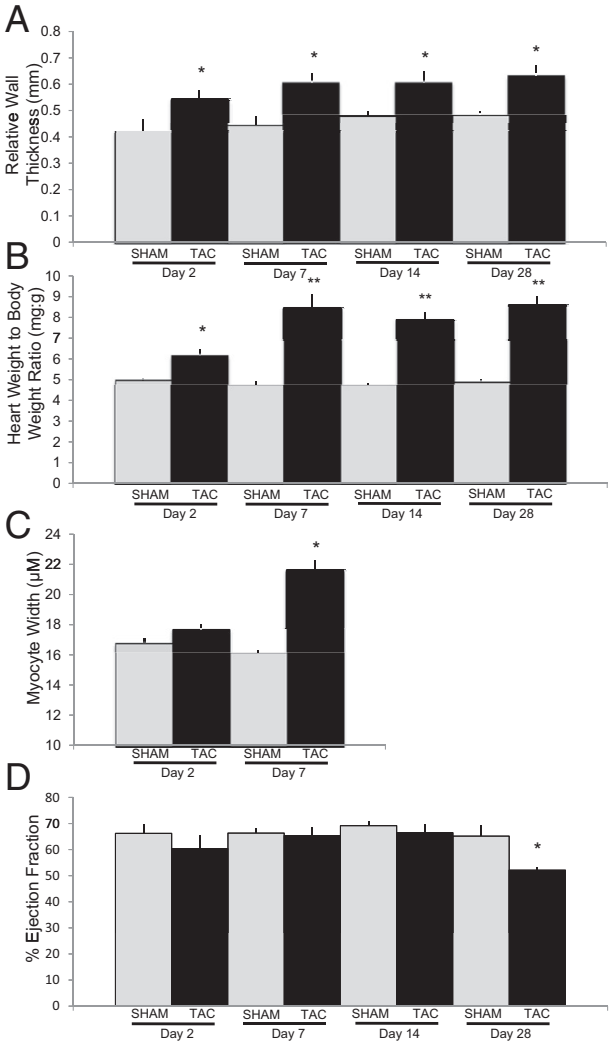

Figure 1. Induction of pressure overload cardiac hypertrophy. Left ventricular wall thickness was increased 2 days after transverse aortic constriction (TAC) and was fully realized by day 7 (**A**), as measured by echocardiography and heart weight (**B**), normalized to body weight. Measurement of myocyte width indicated significant myocyte hypertrophy present 7 days after TAC (**C**). In addition, a trend in lower ejection fraction at day 2 and 28 after TAC was observed (**D**), implying impaired cardiac function at the acute and chronic stages of cardiac hypertrophy. $^{*}P \leq 0.05$ TAC versus sham surgery at the same time point; $^{**}P \leq 0.05$ TAC day 2 versus TAC at other time points. $n \geq 6$.

Examination of cardiac function revealed a lower ejection fraction observed by day 2 and a significant decrease in day 28 TAC hearts (Figure 1D). A decrease in cardiac function (ejection fraction) 28 days after TAC indicates that the hypertrophy observed here progresses into pathological decompensated cardiac hypertrophy. In addition, a lower (albeit not significantly lower) ejection fraction observed 2 days after TAC illustrates the importance of acute cardiac remodeling in response to pathological insult to quickly recover normal cardiac function and maintain

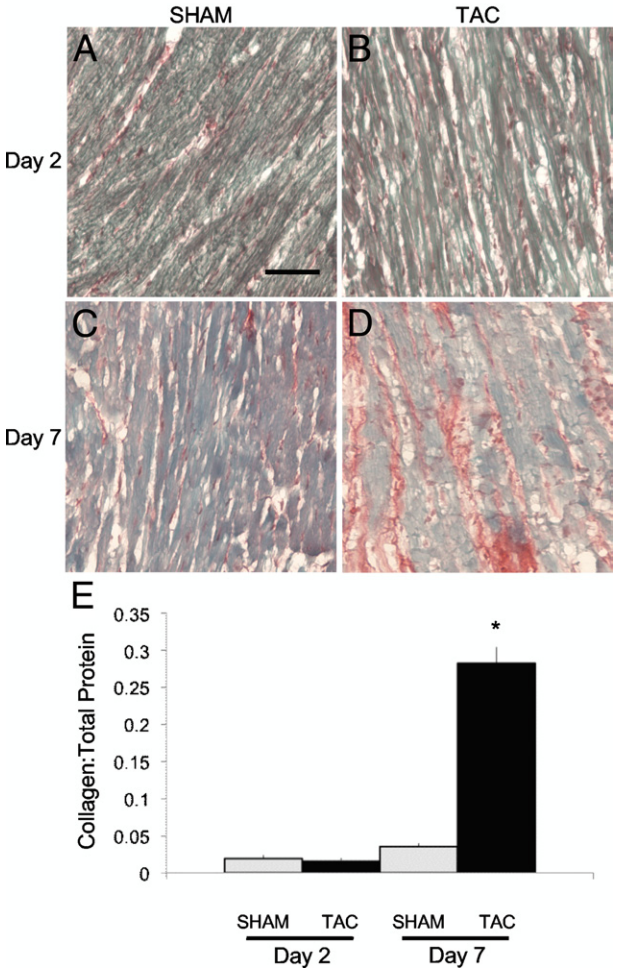

Figure 2. Picrosirius-Fast Green staining revealed a significant increase in collagen deposition 7 days after TAC. Left ventricular and septal regions contained basal levels of collagen in day 2 sham-surgery (**A**) and TAC (**B**) hearts and in day 7 sham-surgery (**C**) hearts, whereas a significant increase in fibrosis was observed in day 7 TAC hearts (**D**). **E:** Collagen measurements were quantified as the ratio of collagen to protein. $^{*}P \leq 0.05$. $n \geq 4$. Scale bar = 25 μm.

cardiovascular output. Given the drastic functional changes that occur within the first week after induction of cardiac stress, we also investigated the morphological changes that occur during this early time period.

Changes in Collagen Deposition in TAC Hearts

In the normal murine myocardium, collagen accounts for very little of the overall tissue, which provides the malleability that the heart requires.[24,25] Approximately 3% of total cardiac tissue was composed of collagen in sham-surgery mice, as indicated by Picrosirius-Fast Green staining (Figure 2, A and C) and quantification (Figure 2E). Similar levels were measured in day 2 TAC hearts, indicating that collagen deposition is not an immediate physiological reaction to pressure overload (Figure 2, B and E). Conversely, a significant increase in collagen deposition was observed in day 7 TAC hearts (Figure 2, D and E), and interstitial fibrosis was evident along with dispersed focal fibrosis throughout the left ventricle and interventricular septum.

Transmission electron microscopy was performed on day 2 and day 7 sham-surgery and TAC hearts and demonstrated a qualitative increase in the amount of collagen and fibroblasts present in TAC hearts, compared with sham-surgery controls (Figure 3). We also qualitatively observed dramatic increases in the mitochondria in myocytes in TAC hearts at both time points. Furthermore, in the TAC samples, the fibroblasts appeared to be more active, with abundant rough endoplasmic reticulum and enlarged Golgi apparatus, indicating high levels of secretion. These data corroborated increased collagen deposition and increased presence of secreted growth factors and cytokines in the TAC hearts.

Given previous studies uncovering a strong functional link between ECM and vascular remodeling, we next examined the course of angiogenesis after TAC surgery.

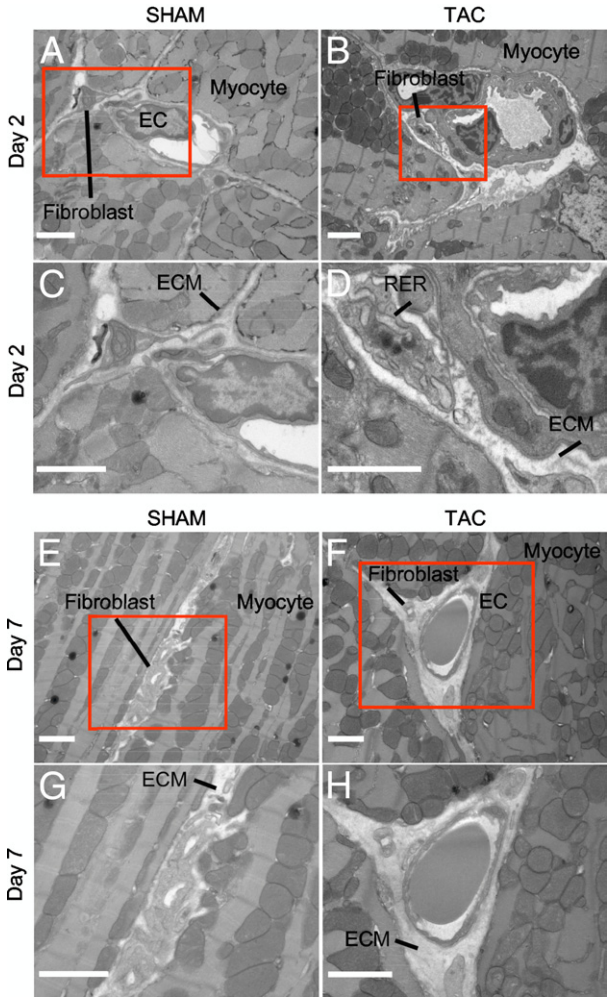

Figure 3. Increased ECM deposition and myocyte hypertrophy in TAC hearts. Transmission electron microscopic images of left ventricular regions in day 2 sham-surgery (**A** and **C**) and TAC (**B** and **D**) hearts and in day 7 sham-surgery (**E** and **G**) hearts revealed similar levels of dense ECM, whereas a significant increase in ECM deposition was observed in day 7 TAC hearts (**F** and **H**). Scale bar = 2 μm.

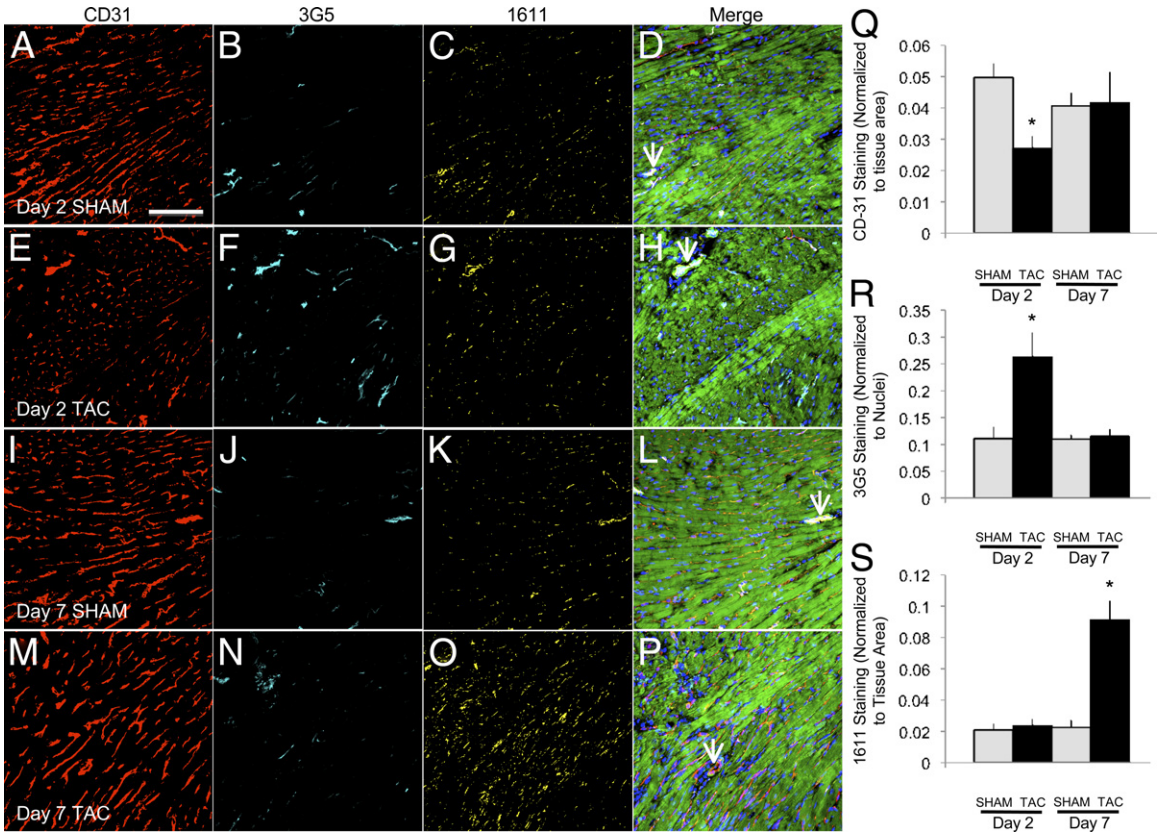

Figure 4. Immunofluorescent staining suggests alterations in cell populations and vasculature in the hypertrophic heart. Immunofluorescent imaging of day 2 sham-surgery (**A**–**D**) and TAC (**E**-**H**) and day 7 sham-surgery (**I**-**L**) and TAC (**M**-**P**) heart sections. CD31 staining (**A**, **E**, **I**, and **M**) and subsequent quantification (**Q**) identified a significant decrease in capillary density in day 2 TAC hearts, which was accompanied by an increase in 3G5-labeled pericytes (**B**, **F**, **J**, **N**, and **R**). The fibroblast-specific marker 1611 demonstrated an increase in the fibroblast cell population in day 7 TAC hearts (**C**, **G**, **K**, **O**, and **S**). The merged images (**D**, **H**, **L**, and **P**) suggest that localization of cells was altered during the early remodeling process. Interestingly, pericytes localized near great vessels (**arrows**) in day 2 sham-surgery and TAC hearts and in day 7 sham-surgery hearts were not present in day 7 TAC samples. In addition, the increased fibroblast population 7 days after TAC localized near capillary beds, suggesting a shift from pericyte-regulated, early vascular regression to fibroblast-mediated capillary growth between days 2 and 7 after TAC. In merged images, F-actin was stained by phalloidin (green); nuclei were stained by DAPI (blue). Scale bar = 100 μm; $n \geq 4$; $^*P \leq 0.05$.

Acute Vascular Remodeling in the Heart After TAC

For long-term survival of the hypertrophic heart, increased vasculature must accompany the myocardial expansion, to maintain tissue health.[26] However, the early vascular changes in response to pathological insult are poorly understood. Immunostaining and subsequent quantification (Figure 4) of the endothelial cell marker CD31 revealed a significant decrease in capillary density just 48 hours after TAC, which returned to sham-surgery levels by day 7 (Figure 4). These data indicate that the first stage of angiogenesis, destabilization of the existing vasculature,[27] occurs within 48 hours after induction of hypertrophy and that the ensuing capillary growth takes place in the days that follow, a time period that also correlates with the observed increase in ECM deposition (Figures 2 and 3).

Pericytes are involved in vascular remodeling after injury in the heart,[28] and their presence represents the end of a window of vascular plasticity.[29] We therefore examined the heart for pericytes during the early remodeling process in response to TAC. A correlation with vascular remodeling was observed, with a significant increase in pericyte association with the vasculature 2 days after TAC, which returned to sham-surgery levels by 7 days (Figure 4). Although previous research using a myocardial infarction model found that pericytes were involved in long-term remodeling,[28] the correlation observed here suggests that pericytes play a role during the acute, early destabilization process and/or immediate reformation of the coronary vasculature in response to injury. Indeed, recent studies suggest that pericytes are attempting to stabilize vessels during the destabilization process,[30] and it may be this balance that facilitates early capillary growth. In addition, great vessels lacked pericyte association only in day 7 TAC hearts (Figure 4), further indicating that large-scale vascular plasticity is present at this time point in TAC animals, but not in the earlier day 2 TAC or sham-surgery animals.

The cardiac fibroblast is another cell that has been identified as an important angiogenic potentiator.[31,32] Immunostaining with the fibroblast-specific antibody 1611[21,22] revealed a close association of fibroblasts with the microvasculature and myocardium under all experimental conditions (Figure 4). However, quantification revealed a significant up-regulation of the fibroblast population 7 days after TAC, which was not observed at the

day 2 time point (Figure 4). Fibroblast-specific staining with 1611 was confirmed by staining with anti-vimentin and anti-DDR2 antibodies (data not shown). As expected, this rise in the fibroblast population is concomitant with fibrosis (Figure 2), but it may also be critical to the angiogenic process in terms of stimulating revascularization of the tissue after the observed early capillary regression.

Cell Proliferation is Altered After Pressure Overload

Given the extensive changes in cardiac cell populations, we analyzed cell proliferation to further infer growth rate and cell origin. In response to injury, new nonmyocyte cells arise within the heart via recruitment of circulating progenitors (fibrocytes), proliferation of resident cells, or differentiation of other cell types.[33,34] To determine the amount of resident cardiac cell proliferation and growth in response to TAC, we analyzed phosphorylated histone H3 (p-histone H3) expression at 2, 7, and 28 days after surgery (Figure 5, A–F). Although significant proliferation and/or growth was observed in the total cardiac cell population at day 2 in TAC hearts, compared with sham-surgery counterparts, a further increase was observed in day 7 TAC hearts (Figure 5G). In addition, the proportion of p-histone H3-positive cells shifted from a 1:1 ratio of myocytes to nonmyocytes to 1:3 by day 7 after TAC, indicating that the increased proliferative rates are due mainly to nonmyocyte populations. Interestingly, both total proliferating cells and the myocyte/nonmyocyte ratio returned to sham-surgery levels by day 28 (Figure 5G).

Changes in Cardiac Cell Populations After TAC

To quantitatively analyze the changes in specific cell populations, we used flow cytometry to measure cell populations in TAC and sham-surgery animals at 3, 7, and 14 days after surgery. In accord with our immunostaining findings, the fibroblast population does not increase until 7 days after TAC, at which point it remains elevated through day 14 (Figure 6). Although it appears that the myocyte population increases, absolute quantities do not actually change, and it is only the percentage that decreases in response to the profound increase in fibroblasts. Also correlating with imaging data is the significant decrease in the endothelial cell population at acute time points (day 2) in response to TAC; this population recovers by day 7 and remains so through day 14 (Figure 6). These data suggest that altered endothelial cell and possibly fibroblast populations contribute to the angiogenic stimulation indicated by early vascular regression followed by vascular regrowth. Interestingly, the unlabeled cell population is increased at the early time point, possibly representing the increase in pericytes observed with immunostaining. However, a further increase in unlabeled cells was present at days 7 and 14, which may indicate undifferentiated infiltrating progenitor cells.

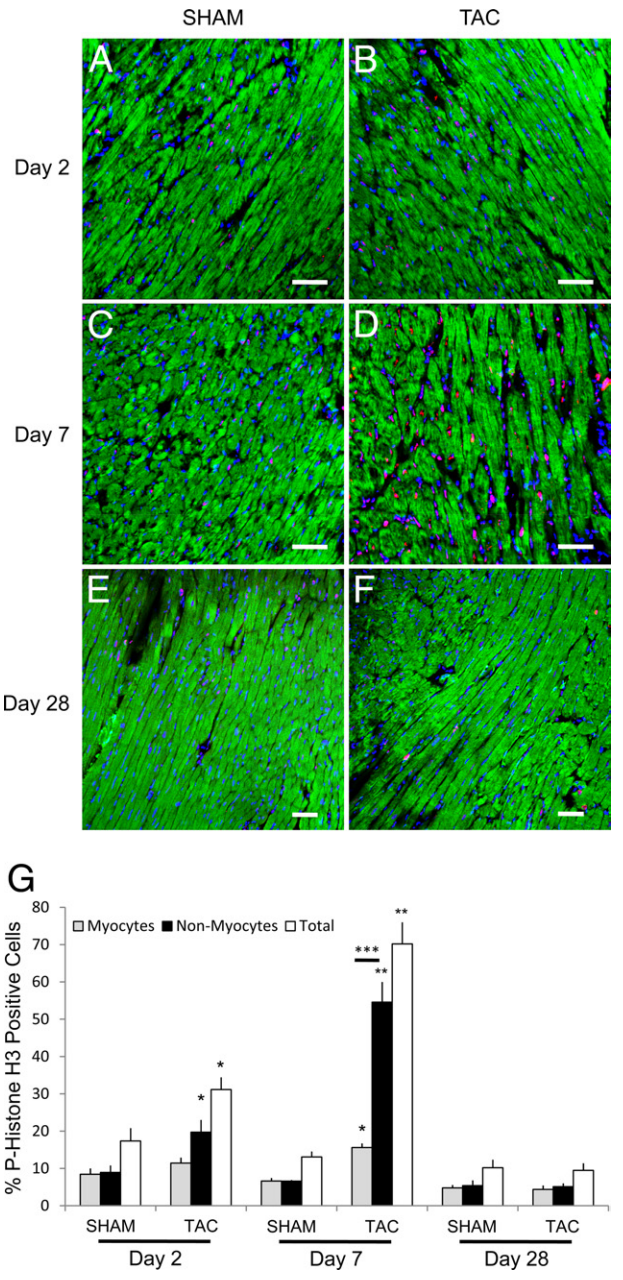

Figure 5. Cell proliferation and growth are induced by pressure overload. Cell growth and proliferation were identified by p-histone H3 staining in left ventricular and septal walls of day 2 sham-surgery (**A**) and TAC (**B**) hearts, day 7 sham-surgery (**C**) and TAC (**D**) hearts, and day 28 sham-surgery (**E**) and TAC (**F**) hearts. Quantification of positive nuclei demonstrated a significant increase in proliferation after 2 days in TAC hearts, which was further augmented by day 7 and then returned back to sham-surgery levels by day 28 (**G**). Although a significant increase in nonmyocyte proliferating cells is present in both day 2 and day 7 TAC mice, no significant number of growing myocytes was present until day 7 in TAC mice, after which numbers returned to sham-surgery levels by day 28 (**E**). In addition, day 7 TAC hearts had significantly more nonmyocyte proliferating cells, compared with day 2 or 28 TAC mice, and consequently had significantly more proliferating nonmyocytes than growing myocytes (**E**), indicating that the increased proliferative rate in day 7 TAC mice is due mainly to expanding of resident nonmyocyte populations. F-actin was stained by phalloidin (green); nuclei were stained by DAPI (blue) and p-histone-positive nuclei were stained pink. $^{*}P \leq 0.05$ in TAC versus sham surgery at the same time point; $^{**}P \leq 0.05$ in TAC day 7 versus TAC at other time points; $^{***}P \leq 0.05$ in myocyte versus nonmyocyte populations. $n \geq 4$. Scale bar = 50 μm.

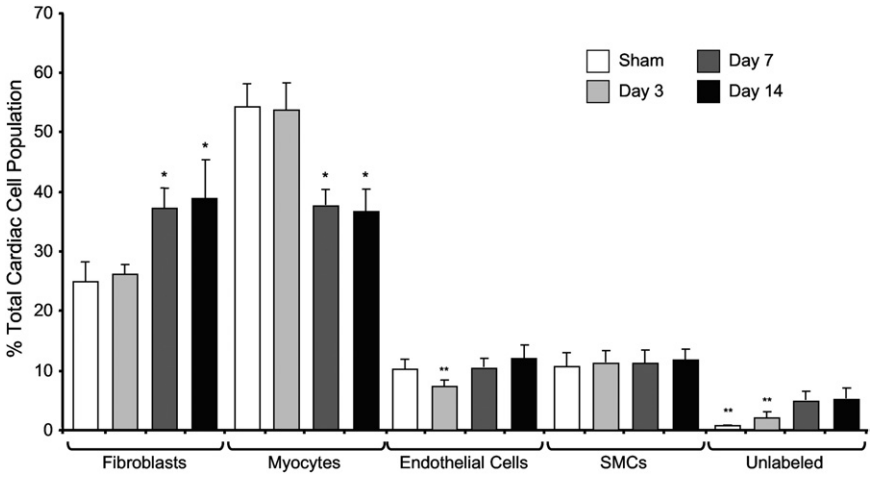

Figure 6. Cell populations in the heart are altered early in response to pressure overload. Fluorescence-activated flow cytometry was used to label and quantify cell populations of the heart at 3, 7, and 14 days after TAC. Equal numbers of cells were analyzed in each group; for percentage calculation, the absolute quantity of cell type was divided by total cells within each sample. $^{*}P \leq 0.05$ versus sham surgery and day 2 TAC; $^{**}P \leq 0.05$ versus all other groups. $n = 4$.

Cardiac Gene Expression is Altered After TAC

To examine possible mechanisms responsible for the observed morphological changes, we measured the expression of 95 genes, using real-time PCR. Genes were grouped into the following categories: cardiac hypertrophy markers, angiogenesis, growth versus differentiation, immune factors, and ECM remodeling. Genes of interest, including those with significant changes, are listed in Table 1. Cardiac hypertrophy markers confirmed that significant hypertrophy was induced in TAC hearts, with a marked increase in the early marker cMYC at days 2 and 7; the late markers ANF and BNP were increased by day 7. In addition, phospholamban (PLN), was down-regulated at day 7, indicative of the initial stages of decompensated cardiac hypertrophy.

As indicated by immunohistochemistry, vascular growth was not induced until 2 days after TAC, as was evident also from the gene expression analyses, with few genes significantly different between TAC and sham-surgery hearts. By day 7, however, TAC hearts had more balanced angiogenic factors, confirmed by a similar capillary density in TAC and sham-surgery hearts. Although several positive angiogenic factors were up-regulated, others were down-regulated, along with an increased expression of the negative regulator Serpinf1. The most apparent pattern of growth and differentiation factors was a notable increase in both processes at day 7. However, the localized growth factor Ereg was highly expressed at day 2, indicating that it may be the early growth-inducing factor, whereas two main differentiation factors, Fzd5 and Lect1, were down-regulated. In accord with previous studies,[35] we found a significant increase in many immune factors early (day 2), but by day 7 these factors were decreased, and their negative regulator, Tgfb2, was increased. One of the more regulated processes at both day 2 and 7 was ECM remodeling, with up-regulated remodeling occurring by day 7. The balance of factors at 2 days after TAC (Ctgf and Thbs1 up-regulated; Lama5, MMP2, and MMP9 down-regulated) may contribute to their role in the angiogenic process at this time point.

Discussion

Traditional dogma states that early ventricular remodeling in response to pathological stimuli is an adaptive process, but that a later, maladaptive period follows.[36] The changes that encompass cardiac remodeling are well defined and include myocyte hypertrophy, fibrosis, and vascular remodeling.[37–39] Although each factor has been targeted for therapeutic intervention, studies have yielded conflicting results. For example, attenuation of myocyte hypertrophy by propranolol treatment improved cardiac function, despite no change in collagen accumulation.[40] The use of a calcimimetic to treat cardiac hypertrophy and remodeling induced by renal failure improved function by decreasing fibrosis and increasing capillary density, whereas left ventricular hypertrophy remained unchanged.[41] Additional studies have identified the induction of angiogenesis as the main determinant of cardiac function, regardless of hypertrophy or fibrosis.[11,42]

It is likely that coordination of these events produces the functional outcome, and here we demonstrate for the first time the early interaction and coordination of morphological changes, cell populations, and gene expression after pathological cardiac insult. Overall cardiac hypertrophy was significant 2 days after TAC and peaked by day 7, and myocyte hypertrophy occurred between days 2 and 7, thus defining the early growth and remodeling phase. Within this phase, we observed several morphological changes, including a sudden increase in fibrosis, extensive vascular remodeling, as well as alterations in cell populations, proliferation, and growth. The time course of the present study allows these events to be correlated with one another, providing valuable insight for future studies of cardiac pathology.

Within 48 hours after induction of pressure overload, the left ventricular free wall and septum significantly enlarged, reflected in an increase in heart weight and rela-

Table 1. Fold Changes in mRNA Gene Expression at 2 and 7 Days after Transverse Aortic Constriction Surgery or Sham Surgery

Regulation of Process	Gene	Day 2 TAC vs sham surgery	Day 7 TAC vs sham surgery	Day 7 TAC vs Day 2 TAC
Angiogenesis				
+	*Angpt1*	−2.658	−2.255*	1.179
+	*Efna1*	−2.638*	−1.332	1.981
+	*Flt1*	1.233*	1.133	−1.088
+	*Hand2*	1.087	−2.954	−3.210*
+	*Hif1a*	−1.096	3.536*	3.876*
+	*Nrp2*	−1.373	1.794	2.462*
+	*Pecam1*	−1.394	1.702	2.374*
+	*Pgf*	−2.131	−2.696*	−1.265
+	*Tek*	−1.270	1.392	1.768*
+	*Vegfa*	−1.299	−1.552	−1.195*
+	*Vegfb*	−1.182	−2.703*	−2.286*
+	*Vegfc*	−1.080	2.143*	2.315*
+	*Vegfd*†	−1.409	2.898*	4.083*
+	*VegfR2*	−1.893*	−1.032	1.835*
−	*Angpt2*	−1.189	1.329	1.580
−	*Serpinf1*	−1.265	7.462*	9.442*
Growth and differentiation				
+	*Egf*	−1.512	−1.312	1.153
+	*Ereg*	22.250*	7.499*	−2.967
+	*Fgf1*	−1.599*	−1.185	1.350
+	*Fgf2*	−1.733*	1.620*	2.808*
+	*Fgf6*	1.060	2.164	2.042
+	*Fgfr3*	1.172	1.390	1.187
+	*Hgf*	3.952	3.806	−1.038
+	*Igf1*	−1.626	3.924*	6.382*
+	*Mdk*	3.037	22.037*	7.257*
+	*Tgfa*	−1.742	11.372*	19.809*
+	*Tgfb1*	−1.089	1.464*	1.594*
+	*Tgfbr1*	−1.204	1.439	1.732
−	*Fzd5*	−2.478*	1.788*	4.430*
−	*Jag1*	−1.189	2.258*	2.684*
−	*Lect1*	−3.605*	−10.001*	−2.774*
−	*Tgfb3*	1.521	4.256*	2.797*
Immune function				
+	*Ccl2*	2.843*	−1.560	−4.434*
+	*Ccl11*	−3.279	−4.032*	−1.230
+	*Cxcl1*	−1.434	1.037	1.487
+	*Cxcl2*	26.822*	−1.003	−26.913*
+	*Cxcl5*	99.814*	1.481	−67.403*
+	*IL1b*	27.274*	3.323	−8.207*
+	*IL6*	41.770*	107.776*	2.580
+	*Tnf*	−1.106	−1.176	−1.063
−	*Tgfb2*	1.393	6.054*	4.347*
Extracellular matrix				
+	*Col18a1*	1.087	3.981*	3.663*
+	*Col4a3*	2.066	−2.911*	−6.015*
+	*Ctgf*	2.854*	15.966*	5.594*
+	*Itgav*	−1.507	3.697*	5.573*
+	*Itgb3*	−1.590	2.422	3.852*
+	*Lama5*	−2.172*	−1.123	1.934*
+	*MMP19*	1.226	−1.259	−1.544
+	*MMP2*	−1.581*	4.963*	7.845*
+	*MMP9*	−3.810*	1.005	3.828*
+	*Thbs1*	2.773*	17.838*	6.432*
+	*Thbs2*	−2.030	4.608*	9.355*
+	*Timp2*	1.036	1.711*	1.652*
+	*Tmprss6*	−2.231	4.490	10.017*

Data are expressed as fold regulation up (+) or down (−).
*$P < 0.05$.
†Synonym for *Figf* (c-fos induced growth factor).
TAC, transverse aortic constriction surgery.

tive wall thickness, compared with sham-surgery counterparts. The ventricular hypertrophy at this time point was not correlated with an increased fibroblast cell population, ECM deposition, or myocyte hypertrophy, indicating that an acute inflammatory response may account for the immediate remodeling (as reflected in the increased heart weight and wall thickness). This notion is supported by our gene expression data and by previous studies

identifying a rise in inflammatory gene expression and cells.[35]

In addition to hypertrophy, a significant decrease in capillary density was observed 2 days after TAC, a time point that was also marked by a significant reduction in the endothelial cell population (other populations remained constant). A decrease in vascular density at this time point may explain the observed decrease in cardiac function, because previous studies have shown that an imbalance of capillary density and hypertrophy causes cardiac dysfunction.[11] A significant increase in pericytes is associated with the reduced capillary density, which may also be reflected by a significant increase in the unlabeled cell population in flow cytometry quantification. Previous research suggests that pericytes are attempting to stabilize vessels and minimize vascular remodeling at this point.[30] Although a decrease in capillary density may appear to be maladaptive, vessel regression is an early step in angiogenesis, important for proper organization of growing capillaries. The participation of pericytes could mark the period in which degradation transitions to new capillary formation and revascularization of the tissue. Clearly, the critical events that define an immediate response to cardiac hypertrophy include an inflammatory response and vascular regression regulated by pericyte infiltration and altered endothelial cell populations, with the fibroblast and ECM morphology remaining relatively unchanged.

The ensuing remodeling process develops entirely new morphological features within the myocardium, reflected in the relative increase in gene expression changes at day 7, compared with day 2. Although development of fibrosis in response to pathology has long been established,[35,38] here we show that it occurs rapidly between days 2 and 7 after induction of pressure overload in mice and is accompanied by a significant increase in the cardiac fibroblast population. Proliferation rates correlated with increased populations of endothelial cells and fibroblasts, and we inferred that resident cardiac cells readily proliferate and contribute to the increased nonmyocyte cell populations observed 7 days after TAC. However, given the timing and transient nature of the pericyte population, it is possible that these cells are recruited from the circulation or are rapidly differentiated.

The combination of fibrosis and increase in nonmyocyte cell populations, along with significant myocyte hypertrophy, contributes to the increased heart weight in TAC mice at day 7, compared with day 2 (Figure 7). Given these results, future studies targeting pathological collagen deposition should focus on this early time period. Indeed, recent studies confirm that fibroblast-mediated changes do not appear until 1 week after pathological stimulation,[17] and here we have shown that these changes take place concurrently with vascular regrowth (because coronary capillary density increased back to sham-surgery levels 7 days after TAC). It is possible that, even though the expanding fibroblast population deposits excess ECM (a maladaptive process that stiffens the heart), it also simultaneously stimulates capillary growth (an adaptive process to deliver more oxygen and nutrients to the expanding myocardium). Given this implication, and in conjunction with the finding of unperturbed proliferative rates 7 days after TAC, regulation of fibroblasts could offer an advantageous route of therapy. In particular, fibroblast turnover seems to be an interesting therapeutic target, because p-histone H3 staining indicates that resident fibroblasts (and other nonmyocyte populations) are rapidly proliferating 7 days after TAC but cell populations remain unchanged through day 14, suggesting that rapid cell proliferation is required to replace cell populations (Figure 7). The decrease in nonmyocyte proliferation by day 28 may also contribute to the transition into cardiac dysfunction, because these populations may be unable to sustain the appropriate levels of turnover and/or activity required to maintain ECM composition and vasculature.

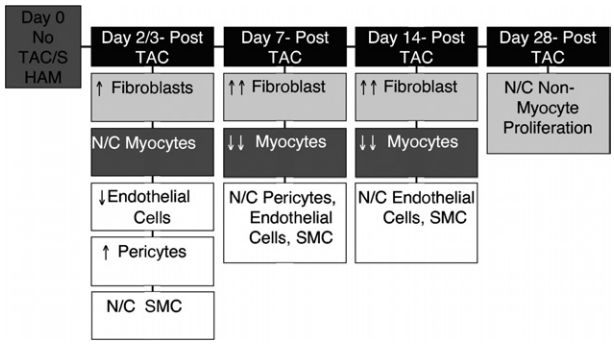

Figure 7. Diagram of cell changes in the heart over a time course after pressure overload in a TAC model. N/C, no change; SMC, smooth muscle cells; TAC, transverse aortic constriction.

Gene expression indicates that the processes of angiogenesis, ECM remodeling, and cell growth are activated concurrently. Separating the two processes of ECM deposition and capillary formation at the early, physiological time point may provide the groundwork for a healthier, functional myocardium during late stages of pathological remodeling. Although the TAC model is an accurate system for portraying remodeling events in the heart,[43] the human response to pressure overload (eg, during hypertension) is obviously more gradual and may vary with respect to specific timing of remodeling. Future studies should examine the remodeling events in a clinical setting. Nonetheless, our present results provide a basis for investigating how these events are coordinated during remodeling and point to the importance of this analysis and possible intervention before pathological remodeling appears.

Acknowledgments

This material is the result of work supported with resources and the use of facilities at the Central Texas Veterans Health Care System, Temple, Texas. We thank Dr. Stephanie L.K. Bowers for production and testing of the 3G5 antibody and Dr. Robert Price and Jeffery Davis (Instrument Resource Facility, University of South Carolina School of Medicine) for their assistance.

References

1. Dorn GW 2nd, Robbins J, Sugden PH: Phenotyping hypertrophy: eschew obfuscation. Circ Res 2003, 92:1171–1175
2. Kaludercic N, Takimoto E, Nagayama T, Feng N, Lai EW, Bedja D, Chen K, Gabrielson KL, Blakely RD, Shih JC, Pacak K, Kass DA, Di Lisa F, Paolocci N: Monoamine oxidase A-mediated enhanced catabolism of norepinephrine contributes to adverse remodeling and pump failure in hearts with pressure overload. Circ Res 2010, 106:193–202
3. Drazner MH: The progression of hypertensive heart disease. Circulation 2011, 123:327–334
4. Goldsmith EC, Borg TK: The dynamic interaction of the extracellular matrix in cardiac remodeling. J Card Fail 2002, 8(6 Suppl):S314–S318
5. Susic D, Varagic J, Frohlich ED: Pharmacologic agents on cardiovascular mass, coronary dynamics and collagen in aged spontaneously hypertensive rats. J Hypertens 1999, 17:1209–1215
6. Weber KT: Fibrosis and hypertensive heart disease. Curr Opin Cardiol 2000, 15:264–272
7. Schwartzkopff B, Motz W, Frenzel H, Vogt M, Knauer S, Strauer BE: Structural and functional alterations of the intramyocardial coronary arterioles in patients with arterial hypertension. Circulation 1993, 88:993–1003
8. Burak M, Frangogiannis NG: The role of TGF-b signaling in myocardial infarction and cardiac remodeling. Cardiovasc Res 2007, 74:184–195
9. Frey N, Olson EN: Cardiac hypertrophy: the good, the bad, and the ugly. Annu Rev Physiol 2003, 65:45–79
10. de Boer RA, Pinto YM, van Veldhuisen DJ: The imbalance between oxygen demand and supply as a potential mechanism in the pathophysiology of heart failure: the role of microvascular growth and abnormalities. Microcirculation 2003, 10:113–126
11. Sano M, Minamino T, Toko H, Miyauchi H, Orimo M, Qin Y, Akazawa H, Tateno K, Kayama Y, Harada M, Shimizu I, Asahara T, Hamada H, Tomita S, Molkentin JD, Zou Y, Komuro I: p53-induced inhibition of Hif-1 causes cardiac dysfunction during pressure overload. Nature 2007, 446:444–448
12. Tribouilloy C, Grigioni G, Avierinos JF, Barbieri A, Rusinaru D, Szymanski C, Ferlito M, Tafanelli L, Bursi F, Trojette F, Branzi A, Habib G, Modena MG, Enriquez-Sarano M; MIDA Investigators: Survival implications of left ventricular end-systolic diameter in mitral regurgitation due to flail leaflets: a long-term follow-up multicenter study. J Am Coll Cardiol 2009, 54:1961–1968
13. Ahmed SH, Clark LL, Pennington WR, Webb CS, Bonnema DD, Leonardi AH, McClure CD, Spinale FG, Zile MR: Matrix metalloproteinases/tissue inhibitors of metalloproteinases: relationship between changes in proteolytic determinants of matrix composition and structural, functional, and clinical manifestations of hypertensive heart disease. Circulation 2006, 113:2089–2096
14. Martos R, Baugh J, Ledwidge M, O'Loughlin C, Murphy NF, Conlon C, Patle A, Donnelly SC, McDonald K: Diagnosis of heart failure with preserved ejection fraction: improved accuracy with the use of markers of collagen turnover. Eur J Heart Fail 2009, 11:191–197
15. van der Meer P, Lipsic E, Henning RH, Boddeus K, van der Velden J, Voors AA, van Veldhuisen DJ, van Gilst WH, Schoebaker RG: Erythropoietin induces neovascularisation and improves cardiac function in rats with heart failure after myocardial infarction. J Am Coll Cardiol 2005, 46:125–133
16. Konstam MA, Kramer DG, Patel AR, Maron MS, Udelson JE: Left ventricular remodeling in heart failure: current concepts in clinical significance and assessment. JACC Cardiovasc Imaging 2011, 4:98–108
17. Stewart JA, Massey EP, Fix C, Zhu J, Goldsmith EC, Carver W: Temporal alterations in cardiac fibroblast function following induction of pressure overload. Cell Tissue Res 2010, 340:117–126
18. Tsujita Y, Muraski J, Shiraishi I, Kato T, Kajstura J, Anversa P, Sussman MA: Nuclear targeting of Akt antagonizes aspects of cardiomyocyte hypertrophy. Proc Natl Acad Sci USA 2006, 103:11946–11951
19. Nakagawa M, Price RL, Chintanawonges C, Simpson DG, Horacek MJ, Borg TK, Terracio L: Analysis of heart development in cultured rat embryos. J Mol Cell Cardiol 1997, 29:369–379
20. Houghton PE, Keefer KA, Diegelmann RF, Krummel TM: A simple method to assess the relative amount of collagen deposition in wounded fetal mouse limbs. Wound Repair Regen 1996, 4:489–495
21. Baudino TA, McFadden A, Fix C, Hastings J, Price R, Borg TK: Cell patterning: interaction of cardiac myocytes and fibroblasts in three-dimensional culture. Microsc Microanal 2008, 14:117–125
22. Bowers SLK, McFadden WA, Borg TK, Baudino TA: Desmoplakin is important for proper cardiac cell-cell interactions. Microsc Microanal 2012, 18:107–114
23. Banerjee I, Fuseler JW, Price RL, Borg TK, Baudino TA: Determination of cell types and numbers during cardiac development in the neonatal and adult rat and mouse. Am J Physiol Heart Circ Physiol 2007, 293:H1883–H1891
24. Weber KT, Sun Y, Tyagi SC, Cleutjens JPM: Collagen network of the myocardium: function, structural remodeling and regulatory mechanisms. J Mol Cell Cardiol 1994, 26:279–292
25. Banerjee I, Fuseler JW, Intwala AR, Baudino TA: IL-6 causes ventricular dysfunction, fibrosis, reduced capillary density, and dramatically alters the cell populations of the developing and adult heart. Am J Physiol Heart Circ Physiol 2009, 296:H1694–H1704
26. Shiojima I, Sato K, Izumiya Y, Schiekofer S, Ito M, Liao R, Colucci WS, Walsh K: Disruption of coordinated cardiac hypertrophy and angiogenesis contributes to the transition to heart failure. J Clin Invest 2005, 115:2108–2118
27. Senger DR, Davis GE: Angiogenesis. Cold Spring Harb Perspect Biol 2011, 3:a005090
28. Ren G, Michael LH, Entman ML, Frangogiannis NG: Morphological characteristics of the microvasculature in healing myocardial infarcts. J Histochem Cytochem 2002, 50:71–79
29. Benjamin LE, Hemo I, Keshet E: A plasticity window for blood vessel remodeling is defined by pericyte coverage of the preformed endothelial network and is regulated by PDGF-B and VEGF. Development 1998, 125:1591–1598
30. Davis GE, Saunders WB: Molecular balance of capillary tube formation versus regression in wound repair: role of matrix metalloproteinases and their inhibitors. J Investig Dermatol Symp Proc 2006, 11:44–56
31. Liu H, Chen B, Lilly B: Fibroblasts potentiate blood vessel formation partially through secreted factor TIMP-1. Angiogenesis 2008, 11:223–234
32. Souders CA, Bowers SLK, Baudino TA: Cardiac fibroblast: the renaissance cell. Circ Res 2009, 105:1164–1176
33. Norris RA, Borg TK, Butcher JT, Baudino TA, Banerjee I, Markwald RR: Neonatal and adult cardiovascular pathophysiological remodeling and repair: developmental role of periostin. Ann N Y Acad Sci 2008, 1123:30–40
34. Nikam VS, Schermuly RT, Dumitrascu R, Weissmann N, Kwapiszewska G, Morrell N, Klepetko W, Fink L, Seeger W, Voswinckel R: Treprostinil inhibits the recruitment of bone marrow-derived circulating fibrocytes in chronic hypoxic pulmonary hypertension. Eur Respir J 2010, 36:1302–1314
35. Ying X, Lee K, Li N, Corbett D, Mendoza L, Frangogiannis NG: Characterization of the inflammatory and fibrotic response in a mouse model of cardiac pressure overload. Histochem Cell Biol 2009, 131:471–481
36. Maisch B: Ventricular remodeling. Cardiology 1996, 87 Suppl 1:2–10
37. Motz W, Strauer BE: Therapy of hypertensive cardiac hypertrophy and impaired coronary microcirculation. J Cardiovasc Pharmacol 1994, 24 Suppl 1:S34–S38
38. Weber KT, Pick R, Jalil JE, Janicki JS, Carroll EP: Patterns of myocardial fibrosis. J Mol Cell Cardiol 1989, 21 Suppl 5:121–131
39. Weber KT, Anversa P, Armstrong PW, Brilla CG, Burnett JC Jr, Cruickshank JM, Devereux RB, Giles TD, Korsgaard N, Leier CV, Mendelsohn FAO, Motz WH, Mulvany MJ, Strauer BE: Remodeling and reparation of the cardiovascular system. J Am Coll Cardiol 1992, 20:3–16
40. Marano G, Palazzesi S, Vergari A, Catalano L, Gaudi S, Testa C, Canese R, Carpinelli G, Podo F, Ferrari AU: Inhibition of left ventricular remodelling preserves chamber systolic function in pressure-overloaded mice. Pflugers Arch 2003, 446:429–436
41. Koleganova N, Piecha G, Ritz E, Bekeredjian R, Schirmacher P, Schmitt CP, Gross ML: Interstitial fibrosis and microvascular disease of the heart in uremia: amelioration by a calcimimetic. Lab Investig 2009, 89:520–530
42. Friehs I, Margossian RE, Moran AM, Cao-Danh H, Moses MA, del Nido PJ: Vascular endothelial growth factor delays onset of failure in pressure-overload hypertrophy through matrix metalloproteinase activation and angiogenesis. Basic Res Cardiol 2006, 101:204–213
43. Hasenfuss G: Animal models of human cardiovascular disease, heart failure and hypertrophy. Cardiovasc Res 1998, 39:60–76